8072 J. Med. Chem. 2010, 53, 8072–8079
DOI: 10.1021/jm1008264

Journal of Medicinal Chemistry Article

Side Chain Cyclization Based on Serine Residues: Synthesis, Structure, and Activity of a Novel Cyclic Analogue of the Parathyroid Hormone Fragment 1−11†

Andrea Caporale,*[,‡] Mattia Sturlese,[‡] Lorenzo Gesiot,[‡] Fabrizio Zanta,[‡,§] Angela Wittelsberger,[∥] and Chiara Cabrele*[,§]

[‡]*Dept. of Chemical Sciences, University of Padova, Institute of Biomolecular Chemistry, CNR, via Marzolo 1, 35131 Padova, Italy,* [§]*Fakultät für Chemie und Biochemie, Ruhr-Universität Bochum, Universitätsstrasse 150, 44801, Bochum, Germany, and* [∥]*Dept. of Physiology, Tufts University School of Medicine, 136 Harrison Avenue, Boston, Massachusetts 02111, United States*

Received July 3, 2010

The N-terminal region of the parathyroid hormone (PTH) is sufficient to activate the G-protein-coupled PTH receptor 1 (PTHR1). The shortest PTH analogue displaying nanomolar potency is the undecapeptide *H*-Aib-Val-Aib-Glu-Ile-Gln-Leu-Nle-His-Gln-Har-NH_2 that contains two helix-stabilizing residues (Aib[1,3]). To increase the helical character and proteolytic stability of this linear peptide, we replaced Gln[6,10] with (a) Lys[6] and Glu[10] to introduce a lactam bridge and (b) Ser[6,10] to form a diester bridge upon cross-linking with adipic acid. These cyclopeptides were, respectively, 468-fold less and 12-fold more potent agonists than the linear analogue. Despite their different potencies, all three analogues adopted similar α-helix structures, as shown by NMR and molecular dynamics studies. However, the diester bridge could better mimic the orientation and chemical properties of the side chains of Gln[6] and Gln[10] in the linear PTH analogue than the lactam moiety. This is apparently important for efficient receptor activation and provides further insights into the receptor-bound ligand conformation.

Introduction

Many cellular processes are controlled by receptor-binding peptides and hormones; therefore, the development of new peptide analogues and peptidomimetics that can target biologically relevant receptors and modulate their activation is of great importance in biology and medicine. Moreover, the prevalence and diversity of bioactive peptides as well as their role in crucial physiological functions have renewed the interest in the application of peptides and peptide derivatives as therapeutic agents.[1,2]

One of the most common strategies to improve the biological activity, proteolytic stability, and pharmacokinetic properties of peptides is based on the introduction of conformational constraints, for example, by backbone or side chain cyclization.[3−9] The nonbiogenic cyclizations via lactam formation between side chains of *ω*-amino and *ω*-carboxyl α-amino acids,[5] via ring-closing metathesis[10−13] of *ω*-alkenyl-containing amino acid building blocks or via click chemistry,[14,15] have been shown to be suitable for the mimicry and stabilization of α-helices that play a major role in mediating ligand−protein and protein−protein interactions. This is especially important in the case of short α-helical segments that possess limited stability due to low nucleation probability.[16,17]

Parathyroid hormone (PTH)[a] is an 84-residue long ligand of the class B G-protein-coupled receptor PTHR1[18] and plays a role in the regulation of Ca^{2+} levels in blood.[19] The N-terminal PTH segment 1−34 maintains full activity[20] and increases bone mineral density and strength; hence, it is considered to be one of the most effective treatments of osteoporosis: As a matter of fact, recombinant PTH-(1−34) (teriparatide) is the first bone formation agent approved for marketing.[21−23]

About a decade ago, Gardella and co-workers found that the N-terminal PTH fragment 1−14 is sufficient to induce PTHR1-mediated cAMP production, but it is a very weak agonist (EC_{50} = 100 μM).[24] However, the following structure−activity relationship (SAR) studies on PTH-(1−14) have led to the identification of analogues with superior potency, such as *H*-[Ala[3,12],Gln[10],homoarginine (Har[11]),Trp[14]]-PTH-(1−14)-NH_2 (EC_{50} = 0.12 μM), and even reduced length, such as *H*-[Ala[3],Gln[10],Har[11]]-PTH-(1−11)-NH_2 (EC_{50} = 3.1 μM).[25] Although the receptor-bound conformation of PTH is not known, structural investigations of PTH-(1−34) indicate the presence of a α-helix starting from residue 3.[26,27] Therefore, the formation of a stable, amphipatic helix should be a prerequisite of the ligand for strong receptor binding and activation. Accordingly, the substitution of native residues with helix-inducing $C^{\alpha,\alpha}$-dialkyl residues resulted in analogues of PTH-(1−11/14) with potencies in the nanomolar range: Examples are *H*-[Aib[1,3],Gln[10],Har[11],Ala[12],Trp[14]]-PTH-(1−14)-NH_2 and *H*-[Aib[1,3],Gln[10],Har[11]]-PTH-(1−11)-NH_2 (EC_{50} = 1.1 and 4.0 nM, respectively).[28] All together, these data support the idea that analogues of the PTH fragments 1−11/14 with improved helix and metabolic stability represent attractive drug candidates for the treatment of osteoporosis.[29] Herein, we propose a chemical approach toward constrained analogues

†Dedicated to Prof. E. Peggion, Department of Chemical Sciences, University of Padova, on the occasion of his retirement.

*To whom correspondence should be addressed. Tel: +39-049-8275740. E-mail: caporaleandrea74@gmail.com (A.C.). Tel: +49-234-3227034. E-mail: chiara.cabrele@rub.de (C.C.).

[a] Abbreviations: Aib, 2-aminoisobutyric acid; CD, circular dichroism; DIPEA, *N*,*N*-diisopropylethylamine; DMF, *N*,*N*-dimethylformamide; Har, homoarginine; HATU, 1-[bis(dimethylamino)methylene]-1*H*-7-azabenzotriazolium hexafluorophosphate 3-oxide; HBTU, 1-[bis(dimethylamino)-methylene]-1*H*-benzotriazolium hexafluorophosphate 3-oxide; HOAt, 1-hydroxy-7-azabenzotriazole; HOBt, 1-hydroxybenzotriazole; Hse, homoserine; Nle, norleucine; NMP, *N*-methyl-2-pyrrolidone; PTH, parathyroid hormone; rPTH, rat PTH; TFA, trifluoroacetic acid; TIS, triisopropylsilane; TMS, tetramethylsilane.

 Published on Web 10/28/2010

of PTH-(1−11), which combines the use of $C^{\alpha,\alpha}$-dialkyl amino acid residues with $i - i + 4$ side chain-to-side chain cyclization via a macrolactam or macrolactone linkage. Their structural and biological properties are presented in the following sections.

Results

Peptide Design and Synthesis. On the basis of a previous study by Gardella and co-workers,[30] there is some evidence that the receptor-bound conformation of PTH displays a close contact between the side chains of the residues at positions 6 and 10. This supports the hypothesis that the N terminus of the ligand must adopt a helical structure upon receptor binding. SAR studies aiming at the minimization of the PTH length showed that substitutions of the native PTH residue Gln^6 are generally not tolerated, whereas the replacement of the native residue Asn^{10} with Gln leads to an analogue with superior potency.[25] Gardella and co-workers[30] investigated the effect of a covalent linkage between the side chains at positions 6 and 10 on the potency of *H*-[$Ala^{3,12}$,Gln^{10},Har^{11},Trp^{14}]-rPTH-(1−14) that was appropriately modified by the substitutions Lys^6/Gln and Glu^{10}/Gln and successively subjected to lactamization. Both the linear and the cyclic forms of the double-substituted analogue are much less potent than the starting analogue (130 and 21 μM, respectively, vs 0.12 μM). However, it is interesting to observe that the cyclic peptide is considerably more potent than the linear one, which suggests that close proximity of the side chains of residues 6 and 10 might favor the binding to the receptor and its activation.

On the basis of the structural and functional data described above and with the aim to find novel small-sized PTH agonists with high potency, we designed two novel analogues of PTH-(1−11) by combining the use of the helix-inducing 2-aminoisobutyric acid (Aib) residues with the side chain-to-side chain cyclization at positions 6 and 10. The Aib-containing linear peptide *H*-[$Aib^{1,3}$,Gln^{10},Har^{11}]-PTH-(1−11)-NH_2, which was previously shown to have nanomolar potency,[28] was chosen as the starting scaffold and was further modified by replacing Met^8 with norleucine (Nle) to avoid sulfur oxidation[31,32] (peptide **1** in Figure 1).

We decided to introduce a cyclic motif by using a lactam bridge between Lys^6 and Glu^{10} (peptide **2**), in analogy to the scaffold previously applied by Gardella and co-workers,[30] or alternatively by cross-linking the side chains of Ser^6 and Ser^{10} with a dicarboxylic acid (peptide **3**). Peptide macrocyclization based on Ser residues has been reported by Grubbs and O'Leary[13] who performed ring-closing metathesis on an α-/3_{10}-helical model heptapeptide[33] containing either *O*-allyl-serine, Ser(All), or *O*-allyl-homoserine, Hse(All), at positions 2 and 6 [Boc-Val-Xaa-Leu-Aib-Val-Xaa-Leu-*O*Me, Xaa = Ser(All) or Hse(All)]. The resulting 21-/23-membered ring system allowed the peptide backbone to adopt a helical conformation similar to that of the linear precursor, although the two-atom shorter ring induced a kink of the helix at the Aib residue. On the basis of this structural study, we opted for a 23-membered cyclic scaffold to prepare the new constrained PTH analogue: Consequently, the side chains of Ser^6 and Ser^{10} were cross-linked by using adipic acid.

Peptide chain assembly was performed by manual solid phase synthesis, using N^{α}-Fmoc-protected amino acids and the coupling reagent mixtures 1-[bis(dimethylamino)methylene]-1*H*-benzotriazolium hexafluorophosphate 3-oxide (HBTU)/1-hydroxybenzotriazole (HOBt)/*N*,*N*-diisopropylethylamine (DIPEA) or 1-[bis(dimethylamino)methylene]-1*H*-7-azabenzotriazolium hexafluorophosphate 3-oxide (HATU)/1-hydroxy-7-azabenzotriazole (HOAt)/collidine.[34,35] The cyclization step was carried out on the solid support as well. For the synthesis of **2**, the alloc and allyl protecting groups were chosen for the side chains of Lys^6 and Glu^{10}, respectively.[36] The peptide chain was assembled until position 6, and then, the alloc and allyl groups were selectively removed with Pd(0) in the presence of phenylsilane as nucleophile. The lactam bridge was formed upon in situ activation with HBTU/HOBt/DIPEA. Then, the peptide chain was further elongated. After acidic cleavage of the crude product from the resin and simultaneous removal of the remaining protecting groups, the purified cyclic peptide was obtained by preparative HPLC and characterized by analytical HPLC and API-TOF-MS (Table 1).

The cyclic analogue **3** was obtained by acylation of the β-hydroxyl groups of Ser^6 and Ser^{10} with adipic acid (Scheme 1). Again, the peptide chain was assembled until position 6. After selective removal of the trityl groups from the Ser side chains with 1% trifluoroacetic acid (TFA) in dichloromethane, the two hydroxyl groups were bridged with adipic acid upon in situ activation with HATU/HOAt/collidine. Unfortunately, the

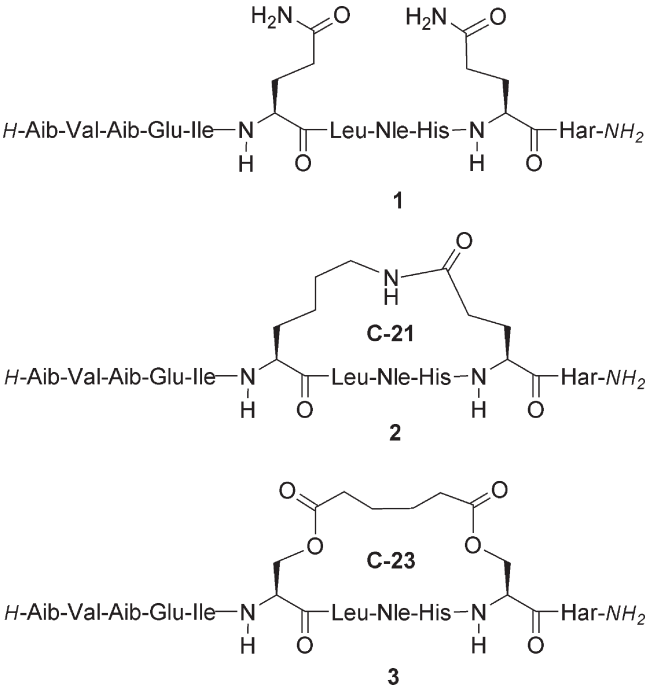

Figure 1. Structures of the linear (**1**) and cyclic (**2** and **3**) analogues of PTH-(1−11).

Table 1. Analytical and Biological Data of the Analogues of PTH-(1−11) **1**−**3**

peptide no.	$M + H_{calcd}^{+a}$ (Da)	$M + H_{obsd}^{+b}$ (Da)	t_R[c] (min)	EC_{50}[d] (nM)
1	1318.8	1318.8	13.2	2.4 ± 0.3
2	1301.8	1301.8	14.0	1122 ± 78
3	1346.8	1346.7	15.0	0.2 ± 0.1

[a] Monoisotopic mass calculated for $M + H^+$. [b] Obtained by API-TOF-MS. [c] Obtained with a gradient of 10−90% B in 20 min (A, 0.1% TFA in water; B, 0.1% TFA in acetonitrile/water 90:10), a flow rate of 1.5 mL/min, and UV detection at 215 nm. [d] Adenylyl-cyclase activity obtained with a luciferase assay on HEK293 cells expressing PTHR1 (the data were obtained by the combination of two independent experiments, each performed in triplicate).

Scheme 1. Synthetic Route for the Preparation of Cyclopeptide **3**

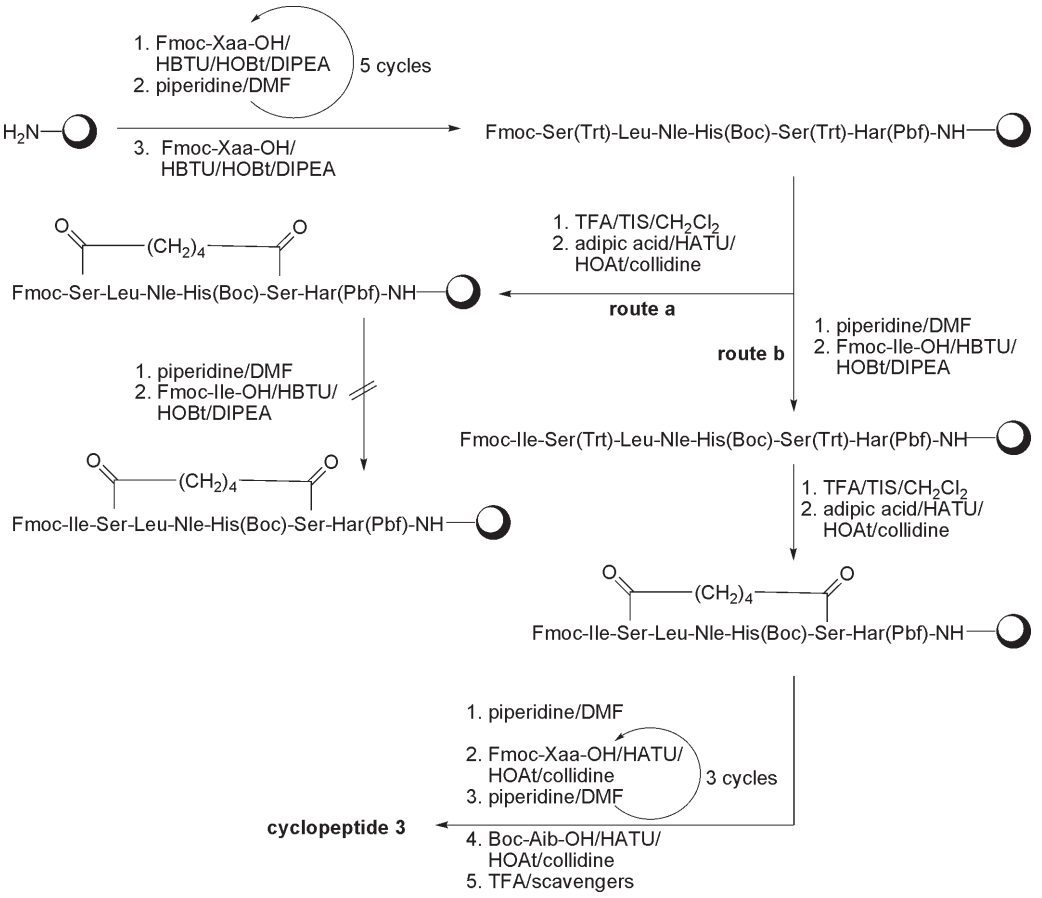

following elongation of the cyclic intermediate with Ile failed, as indicated by persistent positive ninhydrin test[37] despite multiple couplings and confirmed by mass analysis of the peptide obtained by a small-scale TFA cleavage. For this reason, in an alternative synthetic route, the peptide chain was assembled until position 5, followed by selective deprotection/cross-linking of the Ser side chains. After peptide chain elongation and acidic treatment to cleave the resin and the remaining protecting groups, the cyclic peptide **3** was purified by preparative HPLC and identified by analytical HPLC and API-TOF-MS (Table 1).

The linear peptide, used as a reference, was synthesized according to a previous work.[31] The analytical data of the three synthesized peptides are summarized in Table 1.

Circular Dichroism (CD) Spectroscopy. The CD spectra of peptides **1**−**3** were recorded under the same conditions used in previous works for other PTH analogues (TFE/water 20:80, v/v, at 25 °C).[38] The three peptides adopted a helical structure, as indicated by a positive band at 192 nm and two negative ones at 208 and 222 nm (Figure 2). On the basis of the ratio (*R*) of the ellipticity values at 222 and 208 nm, which was close to 0.7 for all three peptides, it could be assumed that both α- and 3_{10}-helix structures were present. Indeed, the *R* value was intermediate between the typical values for α-helices (0.85−0.9) and those for 3_{10}-helices (0.2−0.4).[39] Moreover, it is known that short sequences containing $C^{\alpha,\alpha}$-dialkyl amino acid residues are prone to form a 3_{10}-helix.[40,41] The CD curve of the cyclic analogue **2** containing the lactam bridge between Lys^6 and Glu^{10} was very similar to that of the linear peptide **1**. Its α-helix content was estimated to be 56% by the algorithm CONTIN.[42,43] In contrast, the cyclic analogue **3** containing the bridged residues Ser^6 and Ser^{10} was characterized by a significantly more intense CD

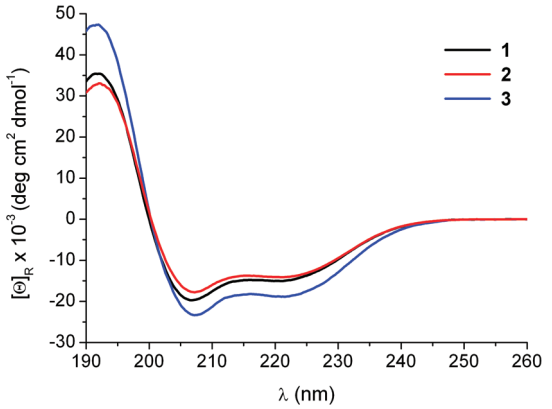

Figure 2. CD spectra of the linear (**1**) and cyclic (**2** and **3**) analogues of PTH-(1−11). The peptide concentration was 200 μM for **1** and **2** and 160 μM for **3** in TFE/water (20:80, v/v).

spectrum, which indicated a superior content of ordered structure with respect to the linear peptide **1** and also to the cyclic peptide **2** (70% α-helix content was estimated[42,43]). No concentration dependency of the CD curves was observed for any of the three analogues (data not shown).

Two-Dimensional (2D) NMR Spectroscopy. The 2D NMR spectra of the three peptides were recorded at the concentration of 2.2 (**1**) or 2.4 mM (**2** and **3**) in TFE/water (20:80, v/v) at 298 and 310 K. The chemical shifts of the linear peptide did not show significant changes at the two temperatures. In contrast, the chemical shifts of the cyclic peptides were found to be temperature-dependent. This observation suggested that the temperature might influence the conformation of the

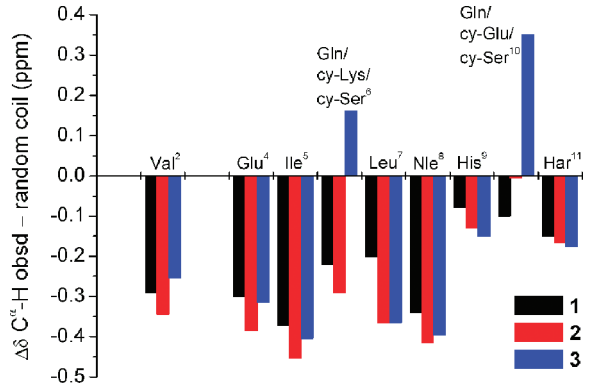

Figure 3. Comparison of the CSI patterns of the linear (**1**) and cyclic (**2** and **3**) analogues of PTH-(1−11). As the temperature effect on the random coil C^{α}-H chemical shifts is negligible in the range of 298−310 K,[48] the chemical shift differences of the C^{α}-H protons were calculated using the corresponding random coil values at 298 K. The prefix "cy" is used for the side-chain cyclized residues.[49]

constrained peptides, which led us to choose the temperature used for the biological tests (310 K) to determine their structures. A complete proton resonance assignment was performed using the standard procedure.[44] The spin systems of all amino acid residues were identified using magnitude correlation spectroscopy (COSY)[45] and CLEAN-total correlation spectroscopy (TOCSY)[46] spectra. The sequence-specific assignment was accomplished using rotating frame Overhauser effect spectroscopy (ROESY)[47] spectra. The peptides were found to adopt an α-helix spanning over residues 2−11, as indicated by the negative pattern of their chemical shift index (CSI) for the C^{α}-H protons (Figure 3). Interestingly, the CSI values of the C^{α}-H protons of the cross-linked residues Ser^6 and Ser^{10} resulted to be positive. This was attributed to the chemical modification of the Ser side chains: Indeed, the conversion of the β-hydroxyl group into an ester group altered the inductive effect of the β-oxygen, leading to a shift of the NMR signals of the C^{α}-H protons toward lower fields. Furthermore, the different extent of the shift observed for the two side-chain acetylated Ser residues was probably due to a difference in the relative orientation between the ester groups and the C^{α}-H protons (diamagnetic anisotropy).

Molecular Dymanics. The structures of peptides **1**−**3** were obtained with a simulated annealing protocol, using the distance restraints extrapolated by the ROE peak intensities (137 for **1**, 158 for **2** and 147 for **3**). Superposition of the 10 best structures of each analogue was characterized by small rmsd values for the backbone-atom positions from Val^2 to cy-Ser/cy-Glu/Gln^{10} (0.282 Å for **1**, 0.207 Å for **2**, and 0.378 Å for **3**), which indicated the presence of a unique conformation for each peptide. In contrast, Har^{11} displayed different possible conformations. The values of the dihedral angles were found to lay in the typical α-helical region of the Ramachandran plot (see the Supporting Information), thus confirming the helix conformation of all three analogues. The side chain cyclization seemed to slightly modify the geometry of the helical segment 4−10: In particular, the distance between the C^{α}-atoms of the cyclized residues at positions 6 and 10 was dependent from the size of the bridge. The average distance calculated for the family of the 10 lower energy structures was 6.42 Å in the reference peptide **1**, whereas it was smaller in peptide **2** (6.22 Å) and higher in peptide **3** (6.71 Å). This implicated a different spatial distribution of the C^{α}-atoms as well as of the side chains. Indeed, the rmsd values for the C^{β}-atoms of peptides **2** and **3** versus the linear peptide **1** were 1.150 and 1.430 Å, respectively.

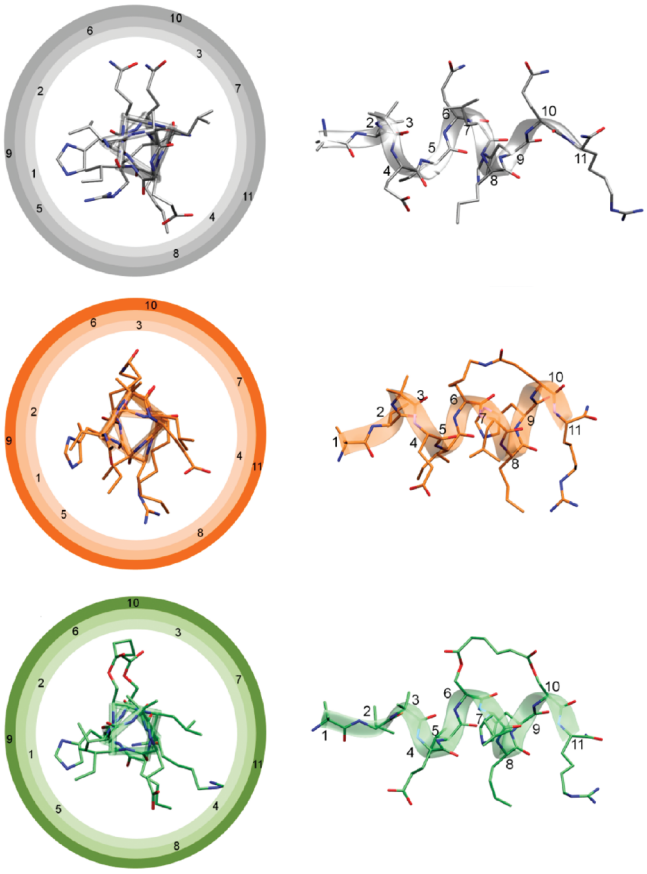

Figure 4. Frontal (left) and lateral (right) view of the lowest energy structures of the linear (**1**) and cyclic (**2** and **3**) analogues of PTH-(1−11) (from the top). In the frontal view, the residue numeration is reported along the C^{α}-atom direction. In the lateral view, the residue number is close to the C^{α}-atom.

Interestingly, the hydrogen bond acceptor character of the two γ-carbonyl groups of Gln^6 and Gln^{10} in peptide **1** was nicely mimicked by the two ester functional groups in analogue **3** (Figure 4). This was obviously not the case of the lactam bridge in analogue **2**, which could display the γ-carbonyl oxygen of the amide group as a single hydrogen bond acceptor. Moreover, the spatial region occupied by the single amide group of the lactam bridge in analogue **2** did not overlap with any of the two regions occupied by the amide groups of Gln^6 and Gln^{10} in analogue **1**.

Biological Activity. The agonistic activity of peptides **1**−**3** was assessed by using a luciferase assay on HEK293 cells stably expressing the PTHR1 (Figure 5). The linear peptide **1** acted as an agonist with an EC_{50} value of 2.4 nM (Table 1). The cyclic analogue **2** was 468-fold less potent than the linear peptide, displaying an EC_{50} value of 1.1 μM. In contrast, the cyclic peptide **3** not only was 12-fold more potent than the linear analogue **1** (EC_{50} = 0.2 nM), but it also showed higher efficacy in activating the receptor, as indicated by the dose−response curve that rose above the 100% activity threshold.

Discussion and Conclusions

Stabilization of the N-terminal helical structure of the PTH fragments 1−11 and 1−14 represents a promising strategy for the development of new antiosteoporosis drugs. In the last years, the most used approach has been the substitution of Ala^1 and Ala^3 with conformationally constrained $C^{\alpha,\alpha}$-dialkyl amino acids like Aib and 1-aminocycloalkane-carboxylic acids.[28,38,50] Moreover, Gardella and co-workers have claimed the presence

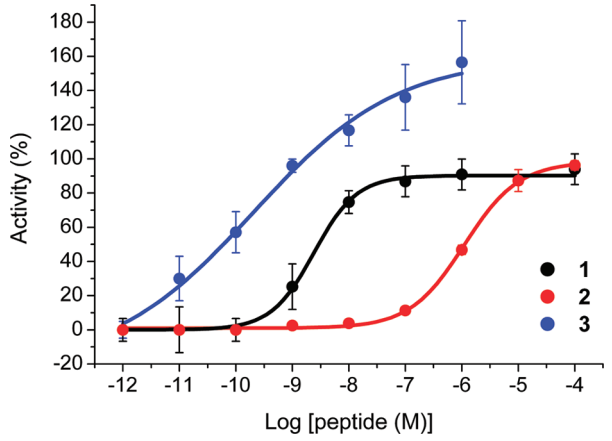

Figure 5. Dose−response curves for the linear (**1**) and cyclic (**2** and **3**) analogues of PTH-(1−11). The values for maximal response and slope were extrapolated by fitting the data with a sigmoidal model. Maximal response: 90 ± 2 (**1**), 98 ± 2 (**2**), and 159 ± 13% (**3**). Slope: 1.1 ± 0.1 (**1**), 0.9 ± 0.1 (**2**), and 0.34 ± 0.10 (**3**).

of close contacts between the side chains of residues 6 and 10 in the receptor-bound conformation of the ligand, being Gln^6 and Asn^{10} in the native PTH sequence.[30] Such a structural motif would correspond to a well-defined α-helix turn, in which the $i - i + 4$ residues would be located on the same face of the amphipatic helix. Therefore, the introduction of a covalent linkage between the $i - i + 4$ side chains is expected to stabilize the α-helix, provided that the chemical and structural changes imposed by the linkage are tolerated. In the case of the N-terminal region of PTH, SAR studies have shown that mutations of Gln^6 are badly tolerated, whereas the substitutions of Asn^{10} with Ala, Asp, Glu, and Gln not only are fully tolerated, but they even enhance the receptor activation in comparison to the unmodified sequence, being Gln^{10}/Asn the most potent mutation.[25] Also, a D-amino-acid scan of the linear analogue **1** underlined the importance of the orientation of the side chain at position 6: Indeed, the D-Gln^6-containing peptide was 40-fold less potent than the D-Gln^{10}-containing one.[31] All together, these observations suggest that both positions 6 and 10, but especially position 6, prefer to be occupied by side chains displaying hydrogen bond donors and/or acceptors.

To improve peptide potency and stability, we have presented here an approach that combines both the advantages deriving from the introduction of conformationally constrained amino acids and the cyclic structures. The cyclic analogue **2** displays a 21-membered macrolactam obtained upon the cyclization of Lys^6 with Glu^{10}. This bridge forces the peptide segment 4−11 to adopt a compact helix motif, as indicated by the minor distance between the C^α-atoms at positions 6 and 10, relative to the linear analogue **1** (6.22 vs 6.42 Å), and as shown in Figure 4. Moreover, although the lactam bridge points into the same direction of the Gln^6 and Gln^{10} side chains in the linear peptide, it is obviously unable to act as surrogate of the two amide groups. This may explain the dramatic loss of potency of cyclopeptide **2** in comparison to the linear peptide reference. Our results confirm the negative effect of the substitution of Gln^6 and Gln^{10} with a lactam bridge between Lys^6 and Glu^{10}, as previously observed for an analogue of PTH-(1−14).[30]

In contrast to the classical lactam formation based on the Lys and Glu/Asp side chains, the cross-linking of two Ser side chains by a dicarboxylic acid offers the possibility to form a bridge of variable length and containing two ester bonds as potential hydrogen bond acceptors. The cyclic analogue **3** presented in this work was obtained by side chain acylation of Ser^6 and Ser^{10} with adipic acid, which results in a 23-membered ring. Although this cyclic motif is just two atoms larger than the lactam bridge, the helix segment 4−11 is significantly less compact than that in the lactam-containing analogue: Indeed, the distance between the C^α-atoms at positions 6 and 10 is 6.71 Å in peptide **3** and 6.22 Å in peptide **2**. Moreover, comparison of the frontal and lateral views of the three peptide structures in Figure 4 clearly shows that the diester bridge is a much better surrogate of the two Gln side chains in peptide **1** than the lactam bridge, as it matches their orientation and additionally mimic the two γ-carbonyl groups. This superior mimicry ability of the Ser-based cyclization reflects the potency of the cyclic analogue **3** that is, respectively, > 5600-fold and 12-fold higher than that of the poor agonist **2** and potent agonist **1**. Interestingly, cyclopeptide **3** produced a greater maximal response than the ligand used as positive control in the luciferase assay, namely, PTH-(1−34)-NH_2. Therefore, the cyclic peptide **3** represents a small-sized, conformationally constrained PTH agonist with subnanomolar potency (0.2 nM) and major efficacy in activating PTHR1-mediated signal transduction in vitro when compared to PTH-(1−34)-NH_2 (activity ratio of about 1.6:1). Such biological properties make of peptide **3** a very interesting PTHR1 ligand, and future investigations will be carried out to deeply understand its mode of receptor binding and activation, which might somehow differ from that of the linear peptide **1**, as the different shape of its dose−response curve, in particular its slope (0.34 against 1), would let presume. To this regard, it has been reported that different PTH analogues may have different affinities for the two putative, pharmacologically distinguishable GTPγS-resistant (R^0) and GTPγS-sensitive (RG) receptor conformations.[51,52] For example, PTH-(1−34), which is hypothesized to interact both with the N-terminal extracellular and transmembrane/extracellular loop domains of the receptor, can almost equally bind both receptor states, whereas *H*-[$Aib^{1,3}$,Gln^{10},Har^{11},Ala^{12},Trp^{14}]-PTH-(1−14)-NH_2, which should interact only with the transmembrane/extracellular loop domain, binds preferentially the RG state.[52] In addition, it has been shown that R^0-preferring ligands produced remarkably prolonged signaling responses in bone and kidney PTH target cells.[52]

In conclusion, we have presented the effect of cyclization of the side chains at positions 6 and 10 on the structure and function of an Aib-containing, linear analogue of PTH-(1−11). The NMR and in vitro studies suggest that the capacity of the ligand to form a stable helix is a structural prerequisite for high receptor activation, provided that other factors, like the presence of key structural/functional groups and their appropriate spatial distribution, are fulfilled. For example, on the basis of this work, the importance of the γ-amide groups of Gln^6 and Gln^{10} seems to be related more with their H-bond acceptor rather than donation function.

Furthermore, the successful design of cyclopeptide **3** shows that side chain-to-side chain cyclization based on the cross-linking of two β-hydroxyl groups with dicarboxylic acids offers a valuable alternative to the commonly used lactam linkages, especially in those cases, in which it is necessary to mimic the presence of two carbonyl groups. The fact that the diester-bridged cyclopeptide **3** is stable in basic buffered aqueous solutions (the peptide degradation in phosphate buffer, pH 8, was 9% after 24 h at room temperature, as detected by HPLC analysis) supports the potential application of such a bridging tool for peptide mimicry.

Experimental Section

Materials and Methods. Rink amide MBHA resin (0.73 mmol/g loading) was obtained from Inalco-Novabiochem (Milan, Italy). HBTU, HOBt, HATU, HOAt, and most of the Fmoc-protected natural amino acids were obtained from GL Biochem (Shanghai, China). Fmoc-Aib-*OH* was purchased from NeoMPs (Strasbourg, France). Collidine was purchased from Carlo Erba Reagenti (Rodano-Milano, Italy). *N*,*N*-Dimethylformamide (DMF) dried over molecular sieves (H_2O < 0.01%) and *N*-methyl-2-pyrrolidone (NMP) were obtained from Iris Biotech GmbH. DIPEA, piperidine, adipic acid, Fmoc-Lys(Alloc)-*OH*, Fmoc-Glu(*O*All)-*OH*, $Pd(PPh_3)_4$, and $PhSiH_3$ were obtained from Fluka (Taufkirchen, Germany). DMEM, fetal bovine serum, Opti-Mem I, and PBS were from Life Technologies, Inc. (Gaithersburg, MD). FuGENE 6 transfection reagent was purchased from Roche Diagnostics (Indianapolis, IN). Passive lysis buffer was from Promega Corp. (Madison, WI). D-Luciferin was obtained from Molecular Probes (Eugene, OR). HPLC peptide purification was performed on a Shimadzu LC-8A instrument (Kyoto, Japan), equipped with a Shimadzu SPD-6A UV detector, using a Waters Delta-Pak silica HPLC column (C_{18}-100 Å, 300 mm × 19 mm, 15 μm). The flow rate was 17 mL/min with a linear gradient of 20−45% (v/v) B over 20 min (A, 0.1% TFA in water; B, 0.1% TFA in 90% acetonitrile/water 90:10). Homogeneity of the products (>95% pure) was assessed by analytical reversed-phase HPLC using a Vydac C_{18} column packed with a polymerically bonded end-capped *n*-octadecyl reversed phase based on 300 Å TP silica (218TP54, 250 mm × 4.6 mm, 5 μm), with a linear gradient of 10−90% (v/v) B in 20 min, a flow rate of 1.5 mL/min and UV detection at 215 nm. Molecular masses were determined on a Perseptive Biosystems MARINER API-TOF mass spectrometer (Foster City, CA) by using the low-flow electrospray mode (instrument resolution/accuracy: 5000/100 ppm) and the external calibration method.

Peptide-Chain Assembly. The synthesis of the linear analogue **1** was previously described.[31] A similar protocol was applied to assemble the C-terminal hexapeptides as precursors for the syntheses of the cyclic analogues **2** and **3** (see the Supporting Information for detailed synthetic schemes). Briefly, peptide chain assembly was performed manually on Rink amide MBHA resin (0.073 mmol). Single couplings (2 h) were carried out with the reaction mixtures Fmoc-Xaa-*OH*/HBTU/HOBt/DIPEA (4:4:4:8 equiv) in DMF, where Xaa was Har(Pbf), Glu(*O*All), Ser(Trt), His(Trt) for peptide **2** or His(Boc) for peptide **3**, Nle, Leu, and Lys(Alloc). The Fmoc group was removed with piperidine/DMF (20:80, v/v) for 45 min.

Peptide 2. The protecting groups alloc and allyl were removed from Lys^6 and Glu^{10} by treating the peptide resin, which had been previously swelled in CH_2C1_2, with a solution of $Pd(PPh_3)_4$ (21 mg, 0.018 mmol, 0.25 equiv) and $PhSiH_3$ (216 μL, 1.75 mmol, 24 equiv) in CH_2C1_2 (2 mL) (3 × 30 min under nitrogen). Then, the peptide resin was washed with CH_2C1_2 (3 × 3 mL, 2 min), DMF (3 × 3 mL, 1 min), and again with CH_2C1_2 (3 × 3 mL, 2 min). Cyclization was performed in NMP/DMF (1:1) (4 mL) by using HBTU (166 mg, 0.44 mmol, 6 equiv), HOBt (59 mg, 0.44 mmol, 6 equiv), and DIPEA (150 μL, 0.88 mmol, 12 equiv) for 2.5 h. This treatment was repeated a second time, and the reaction completion was confirmed by the ninhydrin test. Then, the Fmoc group was removed with piperidine/DMF (1:4) for 45 min, and the peptide chain was elongated by using the reaction mixtures Fmoc-Xaa-*OH*/HATU/HOAt/collidine (4:4:4:8 equiv) in DMF, where Xaa was Ile, Glu(*O*tBu), Aib, and Val. Single couplings (2 h) were used for Ile^5 and Glu^4, whereas double couplings (2 × 2 h) were applied for Aib^3, Val^2, and Aib^1 (the latter was coupled as Boc-protected amino acid).

Peptide 3. After double coupling (2 × 2 h) of Fmoc-Ile-*OH* (4 equiv) with HBTU/HOBt/DIPEA (4:4:8 equiv) in DMF, a small-scale cleavage (5 mg of peptide resin) was carried out with TFA/triisopropylsilane (TIS)/H_2O (95:2.5:2.5) for 2 h, and the cleaved peptide was characterized by MS and analytical HPLC. The data confirmed the high homogeneity of the sequence Fmoc-Ile^5-Ser-Leu-Nle-His-Ser-Har^{11}-NH_2. To cleave the Trt protecting group from the Ser side chains, the peptide resin was preswelled in CH_2Cl_2 and then treated with the mixture TFA/TIS/CH_2Cl_2 (1:5:94) for 2 min. This step was repeated 20 times. Cyclization was carried out in NMP/DMF (1:1) (4 mL) by using adipic acid (7.7 mg, 0.053 mmol, 0.7 equiv), HATU (162 mg, 0.43 mmol, 5.9 equiv), HOAt (58 mg, 0.43 mmol, 5.9 equiv), and collidine (102 μL, 0.77 mmol, 10.5 equiv) for 2 h. This treatment was repeated a second time, and the reaction completion was controlled by analytical HPLC after a small-scale TFA cleavage. After cyclization, the peptide chain was elongated with the remaining amino acids by using the procedure described for peptide **2**.

Peptide Deprotection/Cleavage from the Resin and Purification. The peptide resins were treated with the deprotection and cleavage mixture TFA/TIS/water (95:2.5:2.5) for 2.5 h. After filtration, the crude peptides were recovered by precipitation from methyl *tert*-butyl ether, subjected to preparative HPLC purification, lyophilized, and, finally, characterized by analytical HPLC and API-TOF-MS. All three peptides were >95% pure (based on HPLC analysis). Yields: **1**, 34%; **2**, 4%; and **3**, 7%.

CD Spectroscopy. CD measurements were carried out on a JASCO J-715 spectropolarimeter (Tokyo, Japan). The CD spectra were acquired and processed using the J-700 program for Windows. All experiments were carried out at room temperature using HELLMA quartz cells with Suprasil windows and optical path lengths of 0.01 and 0.1 cm. All spectra were recorded over the wavelength range 190−260 nm, using a bandwidth of 2 nm, a time constant of 8 s, and a scan speed of 20 nm/min. The signal-to-noise ratio was improved by recording eight accumulations. The peptides were dissolved in TFE/water (20:80, v/v), and their concentrations were in the range 0.07−1.07 mM, as estimated by the UV absorbance at 210 nm.[53] The spectra were reported in terms of mean residue molar ellipticity (deg cm^2 $dmol^{-1}$).

2D NMR Spectroscopy. NMR spectra of 2.2 (**1**) or 2.4 mM (**2** and **3**) peptide solutions in TFE/water (20:80, v/v) were recorded at 298 and 310 K on a BRUKER AVANCE DMX-600 spectrometer. The water signal was suppressed by presaturation during the relaxation delay. The spin systems were determined using magnitude-COSY[45] and CLEAN-TOCSY[46] spectra. In the latter case, the spin-lock pulse sequence was 70 ms long. The specific sequence assignment was accomplished by using a ROESY[47] spectrum and a mixing time of 150 ms. All spectra were acquired by collecting 512 experiments, each one consisting of 16 (COSY), 32 (TOCSY), or 56 (ROESY) scans and 2048 data points in the F2 dimension. Spectral processing was carried out using TOPSPIN 1.2. Spectra were calibrated against the tetramethylsilane (TMS) signal. Interproton distances were obtained by integration of the signals from the ROESY spectra after correction of the volumes according to the intensity ratio method.[54] Peak assignment and volumes integration were performed by using the CARA software (downloaded from http://cara.nmr.ch).[55]

Molecular Dynamics. The peptide structures were calculated using X-PLOR-NIH 2.22. The simulated annealing (SA) protocol was performed using r^{-6} averaged values for distances involving equivalent or nonstereo-assigned protons. The SA protocol consisted of two parts: In the first part, 1000 structures for each peptide were obtained by 50 steps of initial energy minimization, followed by 30 ps of high-temperature dynamics at 2000 K and 3000 steps of cooling from 2000 to 100 K. The obtained rough structures were optimized through 200 cycles of energy minimization using a restraint force constant of 50 kcal/(mol Å). In the second part, each structure was refined by heating up to 1000 K and cooling for 20000 steps. Then, the structures were optimized again through 200 cycles of energy minimization. The 10 lower energy structures containing no ROE distance restraints violation (<0.5 Å from the integration value) were chosen for conformational studies. The generated structures were visualized and analyzed using the program VMD (1.8.6.) and MOE2008.10.

Biological Activity. Human embryonic kidney (HEK293) cells stably transfected with recombinant PTHR1 (HEK293/C21 cell line) were used.[56] The cellular cAMP response element (CRE) of luciferase was transfected using the CRE-Luc plasmid. HEK293/C21 cells were cultured at 37 °C in DMEM supplemented with 10% fetal bovine serum in a humidified atmosphere of 95% air and 5% CO_2. The cells were seeded at 10^5 cells/well in 24-well, collagene-coated plates, and on the following day, they were treated with FuGENE 6 transfection reagent (1 μL/well), CRE-Luc plasmid (0.2 μg/well) in 0.5 mL/well Opti-Mem I, serum-free medium, according to the manufacturer's recommended procedure.

Luciferase Assay. About 18 h after CRE-Luc plasmid transfection, the cells were rinsed with PBS, and the transfection medium was replaced with 225 μL/well DMEM. Aliquots of the peptide solutions at different concentrations in PBS supplemented with 0.1% bovine serum albumin were then added to the wells and incubated at 37 °C for 4.5 h. After this time, the medium was aspirated, and the cells were lyzed by gentle shaking with 200 μL/well passive lysis buffer. The cells were transferred to labeled low-binding Eppendorf tubes and centrifuged for 2 min, and then, 80 μL/tube of supernatant was transferred into individual sample glass tubes. The luciferase activity was measured using a Lumat LB 9507 luminometer (EG&G Berthold). All the CRE-Luc experiments were carried out in triplicate. Calculations and data analysis were performed using nonlinear regression.

Acknowledgment. We thank Dr. Thomas Burgemeister (University of Regensburg, Germany), Prof. Stefano Mammi, and the team of the Magnetic Resonance Laboratory CNR-ICB at the University of Padova for their support during the NMR experiments. We are grateful to Dr. Barbara Biondi (University of Padova) for her kind help in mass analysis and to Prof. Stefano Moro and the Molecular Modeling Section of the Department of Pharmaceutical Sciences (Univeristy of Padova) for computational support. We acknowledge Sandhya Sharma for her kind help in the biological tests carried out at the Department of Physiology of the Tufts University School of Medicine, Boston. This work was partly supported by the Deutsche Forschungsgemeinschaft (DFG Grant CA296) and by the Italian Ministry of Education and University.

Supporting Information Available: Schemes of the peptide syntheses, analytical HPLC profiles of the purified peptides, degradation data of cyclopeptide **3** at pH 8 at 25 and 37 °C, tables of the chemical shifts of the peptides and of the random coil C^{α}-H protons used to obtain the CSI patterns, Ramachandran plots of the 10 lower energy structures for each peptide, and summary of the cross-peaks found in the ROESY spectra. This material is available free of charge via the Internet at http://pubs.acs.org.

References

(1) Hruby, V. J. Designing Peptide Receptor Agonists and Antagonists. *Nat. Rev.* **2002**, *1*, 847–858.
(2) Vagner, J.; Qu, H.; Hruby, V. J. Peptidomimetics, a Synthetic Tool of Drug Discovery. *Curr. Opin. Chem. Biol.* **2008**, *12*, 292–296.
(3) Li, P.; Roller, P. P.; Xu, J. Current Synthetic Approaches to Peptide and Peptidomimetic Cyclization. *Curr. Org. Chem.* **2002**, *6*, 411–440.
(4) Hess, S.; Linde, Y.; Ovadia, O.; Safrai, E.; Shalev, D. E.; Swed, A.; Halbfinger, E.; Lapidot, T.; Winkler, I.; Gabinet, Y.; Faier, A.; Yarden, D.; Xiang, Z.; Portillo, P. F.; Haskell-Luevano, C.; Gilon, C.; Hoffman, A. Backbone Cyclic Peptidomimetic Melanocortin-4 Receptor Agonist as Novel Orally Administrated Drug Lead for Treating Obesity. *J. Med. Chem.* **2008**, *51*, 1026–1034.
(5) Harrison, R. S.; Shepherd, N. E.; Hoang, H. N.; Ruiz-Gómez, G.; Hill, T. A.; Driver, R. W.; Desai, V. S.; Young, P. R.; Abbenante, G.; Fairlie, D. P. Downsizing Human, Bacterial, and Viral Proteins to Short Water-stable Alpha Helices That Maintain Biological Potency. *Proc. Natl. Acad. Sci. U.S.A.* **2010**, *107*, 11686–11691.
(6) Hurevich, M.; Tal-Gan, Y.; Klein, S.; Barda, Y.; Levitzki, A.; Gilon, C. Novel Method for the Synthesis of Urea Backbone Cyclic Peptides Using New Alloc-protected Glycine Building Units. *J. Pept. Sci.* **2010**, *16*, 178–185.
(7) Adessi, C.; Soto, C. Converting a Peptide into a Drug: Strategies to Improve Stability and Bioavailability. *Curr. Med. Chem.* **2002**, *9*, 963–978.
(8) Craik, D. J. Seamless Proteins Tie Up Their Loose Ends. *Science* **2006**, *311*, 1563–1564.
(9) Clark, R. J.; Jensen, J.; Nevin, S. T.; Callaghan, B. P.; Adams, D. J.; Craik, D. J. The Engineering of an Orally Active Conotoxin for the Treatment of Neuropathic Pain. *Angew. Chem. Int. Ed.* **2010**, *49*, 6545–6548.
(10) Blackwell, H. E.; Grubbs, R. H. Highly Efficient Synthesis of Covalently Cross-linked Peptide Helices by Ring-closing Metathesis. *Angew. Chem., Int. Ed.* **1998**, *37*, 3281–3284.
(11) Illesinghe, J.; Guo, C. X.; Garland, R.; Ahmed, A.; van Lierop, B.; Elaridi, J.; Jackson, W. R.; Robinson, A. J. Metathesis Assisted Synthesis of Cyclic Peptides. *Chem. Commun.* **2009**, 295–297.
(12) Reichwein, J. F.; Versluis, C.; Liskamp, R. M. Synthesis of Cyclic Peptides by Ring-closing Metathesis. *J. Org. Chem.* **2000**, *65*, 6187–6195.
(13) Blackwell, H. E.; Sadowsky, J. D.; Howard, R. J.; Sampson, J. N.; Chao, J. A.; Steinmetz, W. E.; O'Leary, D. J.; Grubbs, R. H. Ring-closing Metathesis of Olefinic Peptides: Design, Synthesis, and Structural Characterization of Macrocyclic Helical Peptides. *J. Org. Chem.* **2001**, *66*, 5291–5302.
(14) Le Chevalier Isaad, A.; Papini, A. M.; Chorev, M.; Rovero, P. Side-chain-to-side-chain Cyclization by Click Reaction. *J. Pept. Sci.* **2009**, *15*, 451–454.
(15) Cantel, S.; Le Chevalier Isaad, A.; Scrima, M.; Levy, J. J.; DiMarchi, R. D.; Rovero, P.; Halperin, J. A.; D'Ursi, A. M.; Papini, A. M.; Chorev, M. Synthesis and Conformational Analysis of a Cyclic Peptide Obtained via i to i+4 Intramolecular Side-chain-to-side-chain Azide-alkyne 1,3-Dipolar Cycloaddition. *J. Org. Chem.* **2008**, *73*, 5663–5674.
(16) Siedlecka, M.; Goch, G.; Ejchart, A.; Sticht, H.; Bierzynski, A. α-Helix Nucleation by a Calcium-binding Peptide Loop. *Proc. Natl. Acad. Sci. U.S.A.* **1999**, *96*, 903–908.
(17) Yang, J. X.; Zhao, K.; Gong, Y.-X.; Vologodskii, A.; Kallenbach, N. R. α-Helix Nucleation Constant in Copolypeptides of Alanine and Ornithine or Lysine. *J. Am. Chem. Soc.* **1998**, *120*, 10646–10652.
(18) Jüppner, H.; Abou-Samra, A.-B.; Freeman, M.; Kong, X.-F.; Schipani, E.; Richards, J.; Kolakowski, L. F., Jr.; Hock, J.; Potts, J. T., Jr.; Kronenberg, H. M.; Segre, G. V. A G Protein-linked Receptor for Parathyroid Hormone and Parathyroid Hormone-related Peptide. *Science* **1991**, *254*, 1024–1026.
(19) Gardella, T. J.; Jüppner, H. Interaction of PTH and PTHrP with their Receptors. *Rev. Endocr. Metab. Disord.* **2000**, 317–329.
(20) Tregear, G. W.; Van Rietschoten, J.; Greene, E.; Keutmann, H. T.; Niall, H. D.; Reit, B.; Parsons, J. A.; Potts, J. T., Jr. Bovine Parathyroid Hormone: Minimum Chain Length of Synthetic Peptide Required for Biological Activity. *Endocrinology* **1973**, *93*, 1349–1353.
(21) Neer, R. M.; Arnaud, C. D.; Zanchetta, J. R.; Prince, R.; Gaich, G. A.; Reginster, J. Y.; Hodsman, A. B.; Eriksen, E. F.; Ish-Shalom, S.; Genant, H. K.; Wang, O.; Mitlak, B. H. Effect of Parathyroid Hormone (1−34) on Fractures and Bone Mineral Density in Postmenopausal Women with Osteoporosis. *N. Engl. J. Med.* **2001**, *344*, 1434–1441.
(22) Tashjian, A. H., Jr.; Gagel, R. F. Teriparatide [Human PTH-(1−34)]: 2.5 Years of Experience on the Use and Safety of the Drug for the Treatment of Osteoporosis. *J. Bone Miner. Res.* **2006**, *21*, 354–365.
(23) Bukata, S. V.; Puzas, J. E. Orthopedic Uses of Teriparatide. *Curr. Osteoporosis Rep.* **2010**, *8*, 28–33.
(24) Luck, M. D.; Carter, P. H.; Gardella, T. J. The (1−14) Fragment of Parathyroid Hormone (PTH) Activates Intact and Amino-terminally Truncated PTH-1 Receptors. *Mol. Endocrinol.* **1999**, *13*, 670–680.
(25) Shimizu, M.; Potts, J. T., Jr.; Gardella, T. J. Minimization of Parathyroid Hormone. *J. Biol. Chem.* **2000**, *275*, 21836–21843.
(26) Schievano, E.; Mammi, S.; Silvestri, L.; Behar, V.; Rosenblatt, M.; Chorev, M.; Peggion, E. Conformational Studies of Paratathyroid Hormone (PTH)/PTH-related Protein (PTHrp) Chimeric Peptides. *Biopolymers* **2000**, *54*, 429–447.
(27) Jin, L.; Briggs, S. L.; Chandrasekhar, S.; Chirgadze, N. Y.; Clawson, D. K.; Schevitz, R. W.; Smiley, D. L.; Tashjian, A. H.; Zhang, F. Cristal Structure of Human Parathyroid Hormone 1−34 at 0.9 Å Resolution. *J. Biol. Chem.* **2000**, *275*, 27238–27244.
(28) Shimizu, N.; Guo, J.; Gardella, T. J. Parathyroid Hormone (PTH)-(1−14) and -(1−11) Analogs Conformationally Constrained

by α-Aminoisobutyric Acid Mediate Full Agonist Responses via the Juxtamembrane Region of the PTH-1 Receptor. *J. Biol. Chem.* **2001**, *276*, 49003–49012.
(29) Potts, J. T.; Gardella, T. J. Progress, Paradox, and Potential: Parathyroid Hormone Research over Five Decades. *Ann. N. Y. Acad. Sci.* **2008**, *1117*, 196–208.
(30) Shimizu, N.; Petroni, B. D.; Khatri, A.; Gardella, T. J. Functional Evidence for an Intramolecular Side Chain Interaction Between Residues 6 and 10 of Receptor-bound Parathyroid Hormone Analogues. *Biochemistry* **2003**, *42*, 2282–2290.
(31) Caporale, A.; Biondi, B.; Schievano, E.; Wittelsberger, A.; Mammi, S.; Peggion, E. Structure-function Relationship Studies of PTH(1-11) Analogues Containing D-amino Acids. *Eur. J. Pharmacol.* **2009**, *611*, 1–7.
(32) Rosenblatt, M.; Goltzman, D.; Keutmann, H. T.; Tregear, G. W.; Potts, J. T., Jr. Chemical and Biological Properties of Synthetic, Sulphur-free Analogues of Parathyroid Hormone. *J. Biol. Chem.* **1976**, *251*, 159–164.
(33) Karle, I. L.; Flippen-Anderson, J. L.; Uma, K.; Balaram, P. Unfolding of an α-Helix in Peptide Crystals by Solvation: Conformational Fragility in a Heptapeptide. *Biopolymers* **1993**, *33*, 827–837.
(34) Carpino, L. A.; El-Faham, A.; Minor, C. A.; Albericio, F. Advantageous Applications of Azabenzotriazole (Triazolopyridine)-based Coupling Reagents To Solid-phase Peptide Synthesis. *J. Chem. Soc. Chem. Commun.* **1994**, 201–203.
(35) Carpino, L. A.; El-Faham, A.; Albericio, F. Efficiency in Peptide Coupling: 1-Hydroxy-7-azabenzotriazole vs 3,4-Dihydro-3-hydroxy-4-oxo-1,2,3-benzotriazine. *J. Org. Chem.* **1995**, *60*, 3561–3564.
(36) Grieco, P.; Gitu, P. M.; Hruby, V. J. Preparation of "Side-chain-to-side-chain" Cyclic Peptides by Allyl and Alloc Strategy: Potential for Library Synthesis. *J. Pept. Res.* **2001**, *57*, 250–256.
(37) Kaiser, E.; Colescott, R. L.; Bossinger, C. D.; Cook, P. I. Color Test for Detection of Free Terminal Amino Groups in the Solid-phase Synthesis of Peptides. *Anal. Biochem.* **1970**, *34*, 595–598.
(38) Barazza, A.; Wittelsberger, A.; Fiori, N.; Schievano, E.; Mammi, S.; Toniolo, C.; Alexander, J. M.; Rosenblatt, M.; Peggion, E.; Chorev, M. Bioactive *N*-terminal Undecapeptides Derived from Parathyroid Hormone: The Role of α-Helicity. *J. Pept. Res.* **2005**, *65*, 23–35.
(39) Moretto, A.; Formaggio, F.; Kaptein, B.; Broxterman, Q. B.; Wu, L.; Keiderlig, T. A.; Toniolo, C. First Homo-peptides Undergoing a Reversible 3_{10}-Helix/α-Helix Transition: Critical Main-chain Length. *Biopolymers* **2008**, *90*, 567–574.
(40) Toniolo, C.; Polese, A.; Formaggio, F.; Crisma, M.; Kamphuis, J. Circular Dichroism Spectrum of a Peptide 3_{10}-Helix. *J. Am. Chem. Soc.* **1996**, *118*, 2744–2745.
(41) Polese, A.; Formaggio, F.; Crisma, M.; Valle, G.; Toniolo, C.; Bonora, G. M.; Broxterman, Q. B.; Kamphuis, J. Peptide Helices as Rigid Molecular Rulers: A Conformational Study of Isotactic Homopeptides from α-Methyl-α-isopropylglycine, $[$L-(αMe)Val$]_n$. *Chem.—Eur. J.* **1996**, *2*, 1104–1111.
(42) Provencher, S. W.; Glockner, J. Estimation of Globular Protein Secondary Structure from Circular Dichroism. *Biochemistry* **1981**, *20*, 33–37.
(43) Whitmore, L.; Wallace, B. A. Protein Secondary Structure Analyses from Circular Dichroism Spectroscopy: Methods and Reference Databases. *Biopolymers* **2008**, *89*, 392–400.
(44) Wüthrich, K. *NMR of Proteins and Nucleic Acids*; Wiley-VCH: Weinheim, Germany, 1986.
(45) Rance, M.; Sorensen, O. W.; Bodenhausen, G.; Wagner, G.; Ernst, R. R.; Wüthrick, K. Improved Spectral Resolution in COSY 1H NMR Spectra of Proteins via Double Quantum Filtering. *Biochem. Biophys. Res. Commun.* **1983**, *117*, 479–485.
(46) Bax, A.; Davis, D. G. MLEV-17-based Two-dimensional Homonuclear Magnetization Transfer Spectroscopy. *J. Magn. Reson.* **1985**, *65*, 355–360.
(47) Bax, A.; Davis, D. G. Practical Aspects of Two-dimensional Transverse NOE Spectroscopy. *J. Magn. Reson.* **1985**, *63*, 207–213.
(48) Merutka, G.; Dyson, H. J.; Wright, P. E. "Random Coil" ^1H Chemical Shifts Obtained as a Function of Temperature and Trifluoroethanol Concentration for the Peptide Series GGXGG. *J. Biomol. NMR* **1995**, *5*, 14–24.
(49) Caporale, A.; Zanta, F.; Cabrele, C.; Wittelsberger, A.; Peggion, E. Synthesis and Activity of Cyclic Analogues of PTH(1−11). In *Peptides 2008: Chemistry of Peptides in Life Science, Technology and Medicine*; Lankinen, H. Ed.; EPS and FIPS: Helsinki, 2008; pp 72−73.
(50) Shimizu, N.; Dean, T.; Khatri, A.; Gardella, T. J. Amino-terminal Parathyroid Hormone Fragment Analogs Containing α,α-Di-alkyl Amino Acids at Positions 1 and 3. *J. Bone Miner. Res.* **2004**, *19*, 2078–2086.
(51) Dean, T.; Linglart, A.; Mahon, M. J.; Bastepe, M.; Jüppner, H.; Potts, J. T.; Gardella, T. J. Mechanisms of Ligand Binding to the Parathyroid Hormone (PTH)/PTH-related Protein Receptor: Selectivity of a Modified PTH(1−15) Radioligand for G_αS-coupled Receptor Conformations. *Mol. Endocrinol.* **2006**, *20*, 931–943.
(52) Okazaki, M.; Ferrandon, S.; Vilardaga, J.-P.; Bouxsein, M. L.; Potts, J. T.; Gardella, T. J. Prolonged Signaling at the Parathyroid Hormone Receptor by Peptide Ligands Targeted to a Specific Receptor Conformation. *Proc. Natl. Acad. Sci. U.S.A.* **2008**, *105*, 16525–16530.
(53) Tombs, M. P.; Souter, F.; MacLaglan, N. F. The Spectrophotometric Determination of Protein at 210 Millimicrons. *Biochem. J.* **1959**, *73*, 167–170.
(54) Ammalahti, E.; Bardet, M.; Molko, D.; Cadet, J. Evaluation of Distances from ROESY Experiments with the Intensity-Ratio Method. *J. Magn. Reson., Ser. A* **1996**, *122*, 230–232.
(55) Keller, R. *The Computer Aided Resonance Assignment Tutorial*; Cantina Verlag: Goldau, Switzerland, 2004.
(56) Pines, M.; Adams, A. E.; Stueckle, S.; Bessalle, R.; Rashti-Behar, V.; Chorev, M.; Rosenblatt, M.; Suva, L. J. Generation and Characterization of Human Kidney Cell Lines Stably Expressing Recombinant Human PTH/PTHrP Receptor: Lack of Interaction with a *C*-terminal Human PTH Peptide. *Endocrinology* **1994**, *135*, 1713–1716.